A Cartesian adaptive level set method for two-phase flows

By F. Ham AND Y.-N. Young

1. Motivation and objectives

Simulations of flows involving free surfaces have become ubiquitous in the literature. The evolution of both simulation methods and computer speed have allowed the investigation of many problems of increasing complexity and engineering relevance. For 2D simulations, it is reasonably common to use grid resolutions of 512×512 or larger. See for example the 2D planar breaking wave simulations of Chen *et al.* (1999), or the axisymmetric drop breakup simulations of Han and Tryggvason (1999a, 1999b). Many such free surface problems are fundamentally three dimensional and the absence of three-dimensional effects such as the pinch-off of stretched filaments by surface tension makes it difficult to make valid physical conclusions or use 2D results to develop models. Achieving similar grid resolution in 3D, however, is outside the computational reach of most research centers.

For many problems of interest, a fine grid is required in only a relatively small portion of the domain (e.g. around regions of high surface curvature) and much coarser grids are sufficient to capture the smoothly evolving velocity fields far from the surface. It is this type of problem that motivates the present Cartesian adaptive method, where the finest resolution in the neighbourhood of the free surface may be of order 512^3 (sometimes called the effective resolution), but the coarsening away from the free surface yields an actual number of control volumes that is less than using the fine grid everywhere by at least an order of magnitude.

A number of adaptive Cartesian methods for freesurface calculations have been proposed in the literature. For example, Haj-Hariri *et al.* (1997) used Cartesian local grid refinement to investigate thermocapillary motion of 3D drops. Their method used an octree-based structure to store the grid heirarchy. More recently Sussman *et al.* (1999) proposed an adaptive levelset method based on the embedded grid approach, where the global computational domain is divided into uniformly refined rectangular patches. This approach has the advantage of allowing a traditional staggered or semi-staggered structured discretization throughout most of the domain, with special interpolations required only at the interface between grid levels. The embedded grid approach may not, however, lead to the smallest Cartesian grids possible because of the restriction that refined regions be rectangular and isotropic. Additionally, embedded grid approaches can be difficult to parallelize and load balance.

In the present contribution we develop a level set method based on local anisotropic Cartesian adaptation as described in Ham *et al.* (2002). Such an approach should allow for the smallest possible Cartesian grid capable of resolving a given flow. The remainder of the paper is organized as follows. In section 2 the level set formulation for free surface calculations is presented and its strengths and weaknesses relative to the other free surface methods reviewed. In section 3 the collocated numerical method is described. In section 4 the method is validated by solving the 2D and 3D drop oscilation problem. In section

5 we present some results from more complex cases including the 3D drop breakup in an impulsively accelerated free stream, and the 3D immiscible Rayleigh-Taylor instability. Conclusions are given in section 6.

2. Mathematical Formulation

For recent reviews of the level set method and its many applications, the interested reader is referred to Osher and Fedkiw (2001) or Sethian (2001). Here we briefly present its formulation for incompressible 2-fluid problems.

The incompressible, immiscible, two-fluid system is treated as a single fluid with strong variations in density and viscosity in the neighborhood of the interface. The continuity and momentum equations for such a flow can be written in conservative form as:

$$\frac{\partial \rho}{\partial t} + \frac{\partial \rho u_j}{\partial x_j} = 0, \tag{2.1}$$

$$\frac{\partial \rho u_i}{\partial t} + \frac{\partial \rho u_j u_i}{\partial x_j} = -\frac{\partial p}{\partial x_i} + \frac{\partial \tau_{ij}}{\partial x_j} + \rho g_i + \sigma \kappa \delta(d) n_i, \tag{2.2}$$

where u_i is the fluid velocity, ρ the fluid density, p the pressure, τ_{ij} the viscous stress tensor, g_i the acceleration due to gravity, σ the surface tension coefficient, κ the local free surface curvature, δ the Dirac delta function evaluated based on d the normal distance to the surface, and n_i the unit normal at the free surface.

It is well known that solving equations 2.1 and 2.2 directly in the presence of the discontinuities at the interface will lead to the excessive smearing of the interface over long time integration, and/or numerical "ringing" in the region of the discontinuities due to dispersive errors in the numerical discretization. In the present work, we capture the interface as the zero-level isosurface of a higher-order function ϕ, the level set function (effectively an additional transported scalar). On either side of the interface, the sign of the level set function can be used to determine which fluid is present. This allows the fluid properties to be written as a function of the level set only, specifically $\rho = \rho(\phi)$. This allows the continuity equation to be written:

$$\frac{d\rho}{d\phi}\left(\frac{\partial \phi}{\partial t} + u_j \frac{\partial \phi}{\partial x_j}\right) + \rho \frac{\partial u_j}{\partial x_j} = 0 \tag{2.3}$$

For the case of constant density except in the neighborhood of the zero level set, which represents the fluid interface, the solution of the continuity equation can thus be decomposed into the solution of the following:

$$\frac{\partial \phi}{\partial t} + u_j \frac{\partial \phi}{\partial x_j} = 0 \Big|_{\phi=0} \tag{2.4}$$

$$\frac{\partial u_j}{\partial x_j} = 0 \tag{2.5}$$

Eq. 2.4 is the standard evolution equation for the level set function, and eq. 2.5 is the incompressible continuity equation. Note that the level set equation need only be solved near the interface, which we have defined as the zero level set. Away from the interface, it is common to make ϕ equal to a signed distance function.

In a similar way, the application of chain rule to the momentum equation allows the

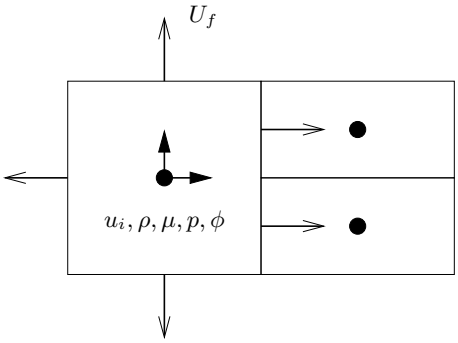

FIGURE 1. Spatial location of variables for collocated discretization.

decomposition of the momentum equation into the solution of the level set equation, eq. 2.4, and the solution of the following momentum equation:

$$\rho\frac{\partial u_i}{\partial t} + \rho\frac{\partial u_j u_i}{\partial x_j} = -\frac{\partial p}{\partial x_i} + \frac{\partial \tau_{ij}}{\partial x_j} + \rho g_i + \sigma\kappa\delta(|\phi|)n_i \tag{2.6}$$

Equations 2.4 – 2.6 comprise our governing system for the present work. Note that the level set formulation results in a system of governing equations that can no longer be written in conservative form. Thus, when the finite volume method is applied to this system, we cannot expect to achieve discrete conservation of mass and momentum (in the region of the interface). It is the hope of the level set formulation that these errors in conservation are mitigated by the more accurate capturing of the interface that is possible with the smoothly-varying level set function.

3. Numerical Method

The governing equations are solved on a Cartesian adaptive grid. The grid arrangement and adaptation are described more completely in Ham *et al.* (2002), and here we only discuss details specific to the simulation of multiphase flows using level set methods on such a grid.

Figure 1 shows the spatial arrangement of variables on the Cartesian adaptive grid. All variables are stored at the control volume (CV) centers with the exception of a face-normal velocity, located at the face centers, and used to enforce the divergence-free constraint in each time step. The variables are staggered in time so that they are located most conveniently for the time advancement scheme. Denoting the time level by a superscript index, the velocities are located at time level t^n and t^{n+1}, and pressure, density, viscosity, and the level set at time levels $t^{n-\frac{1}{2}}$ and $t^{n+\frac{1}{2}}$. The semi-descretization of the governing equations in each time step is then as follows.

Step 1. Advance the level set:

$$\frac{\phi^{n+\frac{1}{2}} - \phi^{n-\frac{1}{2}}}{\Delta t} + u_j^n \frac{1}{2}\frac{\partial}{\partial x_j}\left(\phi^{n-\frac{1}{2}} + \phi^{n+\frac{1}{2}}\right) = 0 \tag{3.1}$$

Here the advantage of time-staggering is evident – i.e. we know the velocity u_i^n from the previous time step, so this equation is decoupled from the other equations, and can be advanced on its own to get the level set value at the mid-point of the new time level, $\phi^{n+\frac{1}{2}}$. Here we have used an implicit Crank-Nicholson time advancement scheme, which requires an iterative solution method. In practice the hyperbolic system is not stiff, and can be quickly converged by a simple iterative scheme such as Gauss-Seidel. The spatial derivatives required in eq. 3.1 are approximated by a 5^{th}-order WENO scheme (Jiang & Peng 2000). While effective at recovering the viscosity solution to the level set equation, the WENO discretization requires that the grid be locally refined in a uniform way in a band about the zero level set, and thus does not take full advantage of the flexibility in the adaptive grid.

Step 2. Reinitialize the level set by solving to steady state:

$$\frac{\partial \phi}{\partial \tau} = sgn\left(\phi\right)\left(1 - \left|\nabla \phi\right|\right). \tag{3.2}$$

The reinitialization step is performed every time step, and ensures that the level set is a signed distance function away from $\phi = 0$, without (theoretically) changing the location of the zero-level set. Spatial derivatives required in eq. 3.2 are once again approximated using a 5^{th}-order WENO scheme (Jiang & Peng 2000). For this equation we use explicit third order TVD Runge-Kutta method for time integration. In practice, it is not neccessary to solve to steady state, and we have found that 5 iterations with a pseudo-time step of $\Delta\tau = \Delta x/4$ is sufficient when performed every computational time step.

Step 3. Calculate the new density and viscosity at the midpoint of the time step:

$$\rho^{n+\frac{1}{2}} = \rho_1 H\left(\phi^{n+\frac{1}{2}}\right) + \rho_2\left(1 - H\left(\phi^{n+\frac{1}{2}}\right)\right) \tag{3.3}$$

$$\mu^{n+\frac{1}{2}} = \mu_1 H\left(\phi^{n+\frac{1}{2}}\right) + \mu_2\left(1 - H\left(\phi^{n+\frac{1}{2}}\right)\right) \tag{3.4}$$

where ρ_1, μ_1 are the constant properties of the fluid occupying the region $\phi > 0$, and ρ_2, μ_2 are the constant properties of the fluid occupying the region $\phi \leq 0$, and H is a smoothed Heaviside step function (Sussman *et al.* 1994).

Step 4. Project the momentum equations:

The remaining steps are a variant of the collocated fractional step method described, for example, by Kim and Choi (2000). First, calculate a projected velocity field $\hat{u}_i$ using the momentum equations:

$$\frac{\hat{u}_i - u_i^n}{\Delta t} = -\frac{1}{\rho^{n+\frac{1}{2}}}\left(\frac{\partial p}{\partial x_i}^{n-\frac{1}{2}} + R_i^{n+\frac{1}{2}}\right) \tag{3.5}$$

where R_i contains all other terms in the momentum equation, eq 2.6. We discretize both the convective and viscous terms implicitly using second-order symmetric discretizations, and the surface tension explicitly based on the known level set at the midpoint of the current time step, $\phi^{n+\frac{1}{2}}$. Some care must be taken in the discretization of the surface tension terms when treated as source terms in the momentum equations of a collocated scheme, as described below.

Step 5. Subtract the old pressure gradient:

$$u_i^{*n+1} = \widehat{u}_i^{n+1} + \Delta t \frac{1}{\rho^{n+\frac{1}{2}}} \frac{\delta p}{\delta x_i}^{n-\frac{1}{2}} \tag{3.6}$$

Step 6. Interpolate the starred velocity field to the faces:

$$U_f^{*n+1} = \overline{u_i^{*n+1}}^f - \Delta t \left(\overline{\frac{R_i^{n+\frac{1}{2}}}{\rho^{n+\frac{1}{2}}}}^f - \frac{R_f^{n+\frac{1}{2}}}{\rho_f^{n+\frac{1}{2}}} \right), \tag{3.7}$$

where $\overline{()}^f$ is a second-order interpolation operator that yields a face-normal component from two CV-centered vectors.

Step 7. Solve the variable coefficient Poisson equation for the new pressure:

$$\frac{1}{\Delta t} \sum_f U_f^{*n+1} A_f = \sum_f \frac{1}{\rho_f^{n+\frac{1}{2}}} \frac{\delta p}{\delta n}^{n+\frac{1}{2}} A_f. \tag{3.8}$$

Step 8. Update the face velocities to the new divergence-free field:

$$\frac{U_f^{n+1} - U_f^*}{\Delta t} = -\frac{1}{\rho_f^{n+\frac{1}{2}}} \frac{\partial p}{\partial n}^{n+\frac{1}{2}} \tag{3.9}$$

Step 9. Reconstruct the pressure gradient at the CV centers:

$$\frac{1}{\rho^{n+\frac{1}{2}}} \frac{\partial p}{\partial x_i}^{n+\frac{1}{2}} = \overline{\frac{1}{\rho_f^{n+\frac{1}{2}}} \frac{\partial p}{\partial n}^{n+\frac{1}{2}}}^{x_i} \tag{3.10}$$

where $\overline{()}^{x_i}$ represents a reconstruction operator. In this case we use a face-area weighted least squares reconstruction.

Step 10. Update the CV velocities:

$$\frac{u_i^{n+1} - u_i^*}{\Delta t} = -\frac{1}{\rho^{n+\frac{1}{2}}} \frac{\partial p}{\partial x_i}^{n+\frac{1}{2}} \tag{3.11}$$

By adding eqs. 3.5, 3.6, and 3.11, it is clear that a second-order time advancement of the momentum equation is recovered.

A critical difference between the present formulation and the formulation of Kim and Choi is in the calculation of the starred face-normal velocities (eq. 3.7). Kim and Choi assume that:

$$\overline{\frac{R_i^{n+1/2}}{\rho^{n+1/2}}}^f \approx \frac{R_f^{n+1/2}}{\rho_f^{n+1/2}}. \tag{3.12}$$

This is an $O(\Delta x^2)$ approximation, seemingly consistent with the overall accuracy of the method, and significantly simplifies the calculation of the Poisson equation source term. In the present investigation, however, it was found that when surface tension forces were introduced in the region of the zero level set, this approximation could lead to large non-physical oscillations in the CV-centered velocity field. To solve this problem, the surface tension forces must be calculated at the faces, and then averaged to the CV centers, i.e.:

$$\frac{R_i^\sigma}{\rho} \equiv \overline{\frac{R_f^\sigma}{\rho_f}}^{x_i} \tag{3.13}$$

With this calculation of the surface tension forces, we can no longer make the assumption of eq. 3.12, and the additional terms must be included in the calculation of U_f^* and thus in the Poisson equation source term.

4. Validation

As validation cases for the method, we solve the 2D column and 3D drop oscillation problems.

4.1. *2D column oscillation*

From Lamb (1932), for a 2D column of liquid in the limit of zero viscosity perturbed according to:

$$r = a\left(1 + \varepsilon cos\left(n\theta\right)\right) \tag{4.1}$$

where a is the mean radius, ε a small perturbation, and n the mode, the oscillation frequency will be:

$$\omega^2 = n\left(n^2 - 1\right)\frac{\sigma}{\rho a^3}. \tag{4.2}$$

Figure 2(a) shows the initial condition for a drop oscillation calculation for mode $n = 5$. Here we have exaggerated the perturbation amplitude to $\varepsilon = 0.15$ for illustrative purposes. In the actual computations, $\varepsilon = 0.02$ was used for the initial condition. Figure 2(b) compares the calculated results to the theory (period $T = 2\pi/\omega$), with generally good agreement. For these calculations, we used periodic boundary conditions in a square domain of size $L = 4a$, and set the density of the surrounding fluid to $\rho_2 = 0.001\rho$ to minimize its effect on the oscillations. The fluid viscosity was adjusted to keep the decay in amplitude of the oscillations to less that 5% per cycle.

4.2. *3D drop oscillation*

For a 3D drop perturbed according to

$$r = a\left(1 + \epsilon S_n\right) \tag{4.3}$$

where the surface harmonics of order n, S_n, are defined:

$$S_1 = \frac{1}{2}\sqrt{\frac{3}{\pi}} cos\theta \tag{4.4}$$

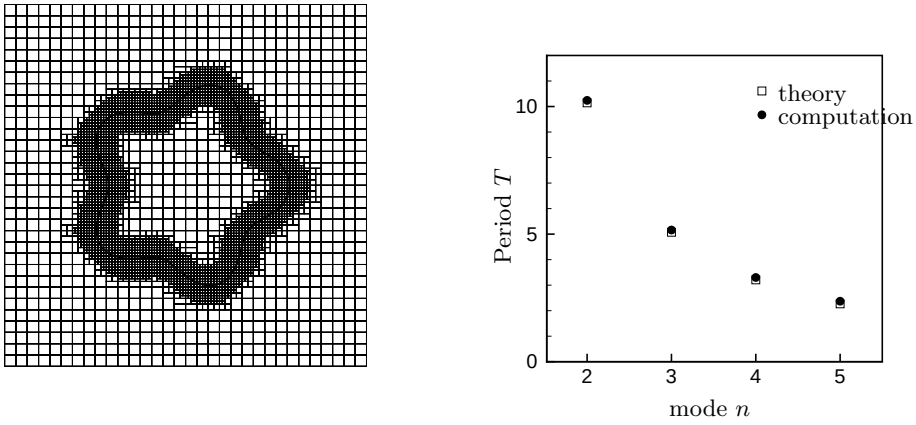

(a) (b)

FIGURE 2. a) Sample grid and initial zero-level set for 2D drop oscillation problem with $n = 5$. b) Comparison of computed and theoretical 2D drop oscillation periods for modes $n = 2$ through 5.

$$S_2 = \frac{1}{4}\sqrt{\frac{5}{\pi}}\left(3cos^2\theta - 1\right) \tag{4.5}$$

$$S_3 = \frac{1}{4}\sqrt{\frac{7}{\pi}}\left(5cos^3\theta - 3cos\theta\right) \tag{4.6}$$

$$S_4 = \frac{3}{16}\sqrt{\frac{1}{\pi}}\left(35cos^4\theta - 30cos\theta + 3\right) \tag{4.7}$$

$$S_5 = \frac{1}{16}\sqrt{\frac{11}{\pi}}\left(63cos^4\theta - 70cos^2\theta + 15\right) \tag{4.8}$$

the oscillation frequency is given by:

$$\omega^2 = n\left(n-1\right)\left(n+2\right)\frac{\sigma}{\rho a^3}. \tag{4.9}$$

Figure 3 (a) shows the drop surface for the mode $n = 5$. Figure 3 (b) compares the calculated results to the theory, also with good agreement.

5. Results

In the following subsections we present some results from simulations of more complex flows. For the purposes of this paper describing the numerical method, these cases are meant to simply illustrate the potential of the method. Consequently we do not present any analysis of the associated flow physics, which will be the subject of future investigations.

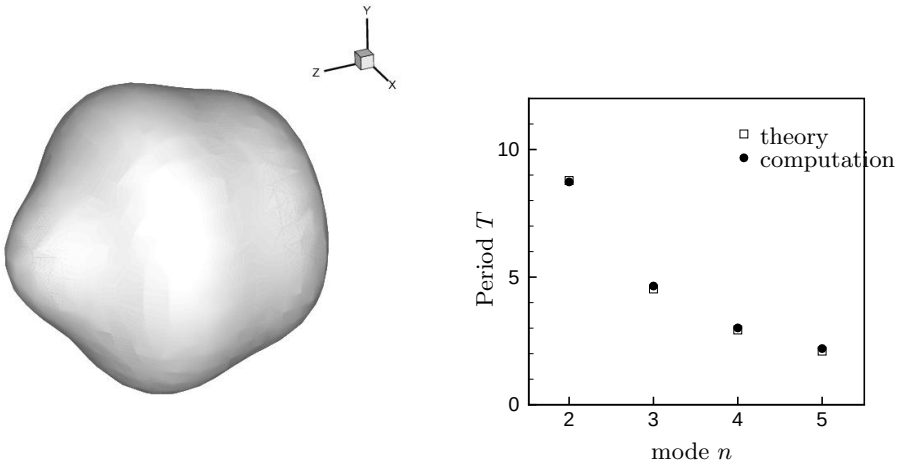

FIGURE 3. a) Initial zero-level set for 3D drop oscillation problem with $n = 5$. b) Comparison of computed and theoretical 3D drop oscillation periods for modes $n = 2$ through 5.

5.1. *Secondary breakup of spherical drops*

The secondary breakup of drops is an important problem in spray atomization, and the subject of the 2D axisymmetric numerical investigation of Han and Tryggvason (1999a, 1999b). We used the present Cartesian adaptive method to calculate 3D drop breakup in an impulsively accelerated free stream. Figure 4 shows the calculated free surface for a case run with equivalent resolution of $128\times128\times128$ with a domain size of $5D\times5D\times5D$.

5.2. *Rayleigh-Taylor Problem*

The Rayleigh-Taylor instability refers to the instability of the plane interface between two fluids of different density superimposed one over the other and subject to gravity. When the upper fluid has a density greater than the lower fluid, the interface can be unstable to small perturbations whose amplification is well described by linear theory with dependence on the density ratio, gravity, surface tension coefficient, and viscosity (Chandrasekhar 1961). As the amplification continues and the problem enters the nonlinear regime, the fluid mixing can become chaotic, characterized by bubbles of lighter fluid rising into the heavier fluid, and spikes of heavier fluid falling into the lighter fluid, with regions of high vorticity near the spike/bubble interface. The resulting mixing zone is known experimentally (Schneider *et al.* 1998) to broaden in a way that depends linearly on the gravitational acceleration g and the Atwood number $A = (\rho_1-\rho_2)/(\rho_1+\rho_2)$, and quadratically on the time, i.e.

$$h_{b,s} = \alpha_{b,s} A g t^2, \tag{5.1}$$

where h_b or h_s represents the penetration length for bubbles or spikes respectively, and α has been introduced as a constant of proportionality, sometimes called the acceleration constant.

Recently, the miscible Rayleigh-Taylor problem has been investigated numerically by

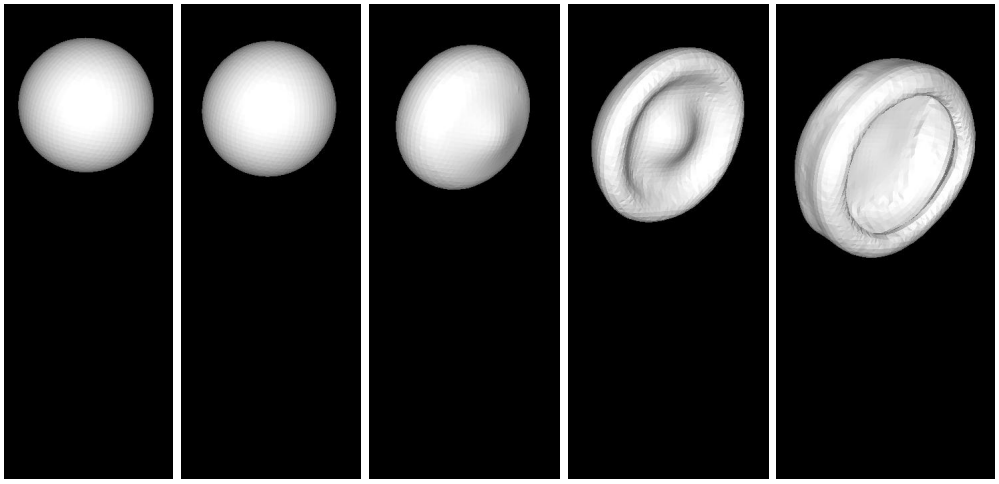

(a) 0.5 (b) 1.5 (c) 2.5 (d) 3.5 (e) 4.5

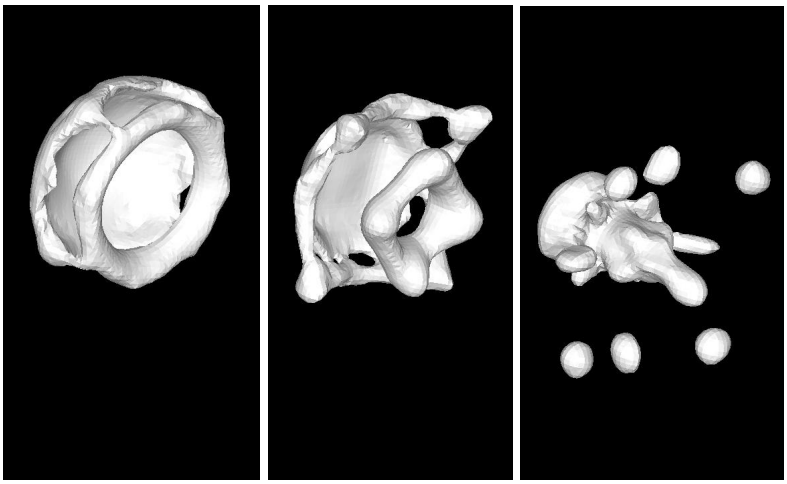

(f) 5.5 (g) 6.5 (h) 8.5

FIGURE 4. Breakup of an initially spherical drop in an impulsively accelerated field. The number below each figure indicates the non-dimensional time tU/D. Free stream velocity is from top-left-back to lower-right-front. Properties for this simulation are as follows: $Re = \rho_g DU/\mu_g = 1000$, $We = \rho_g U^2 D/\sigma = 20$, $Oh = \mu_l/\sqrt{\rho_l \sigma D} = 0.007$.

Young *et al.* (2001), who calculate $\alpha_b \approx 0.03$. Experimental results for immiscible fluids yield higher values of $\alpha_b \approx 0.05 - 0.07$. A recent review of experimental and simulation results for the immiscible case is given by Glimm *et al.* (2001).

Figure 5 presents some results from the application of the present Cartesian adaptive method to this problem. These computations were performed in a $2 \times 2 \times 2$ box with the interface perturbed randomly with a maximum amplitude of 0.01. Properties of the simulation were selected to give a wavelength of maximum instability of $\lambda^* = 0.35$. These

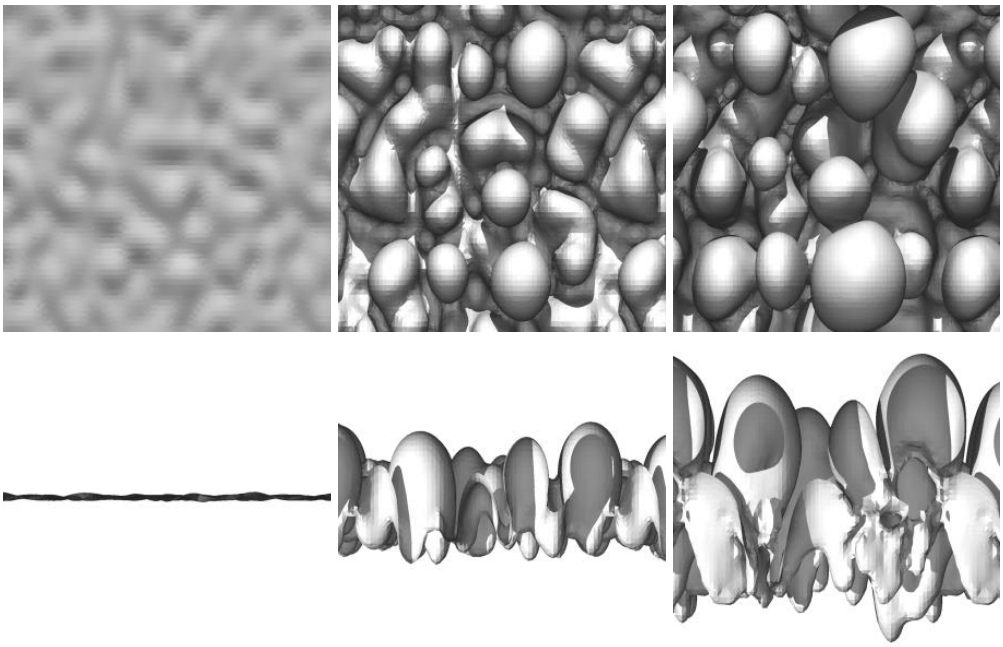

FIGURE 5. Evolution of the interface for the 3D Rayleigh-Taylor problem with multi-mode perturbation: top panels – plan view looking down on interface; bottom panels – elevation view from side.

preliminary simulations were made with the relatively coarse equivalent resolution in the region of the zero-level set of $64 \times 64 \times 64$, or about 10 CVs per wavelength for the most unstable mode. Figure 5 illustrates the evolution of the interface at 3 different times for the Atwood number $A = 0.98$.

6. Conclusions

A simulation tool that integrates Cartesian adaptive grids with the level set method has been developed. The method as described is particularly suited to problems where the smallest scales are associated with the free surface motions, and significant savings can thus be realized by coarsening the grid away from the surface. The method has been validated and its potential demonstrated by solving several test problems, including 2D and 3D drop oscillations, drop breakup in an impulsively accelerated free stream, and the immiscible 3D Rayleigh-Taylor problem.

Our ongoing work is focused on changing the level set solver to the particle level set method of Enright *et al.* (2002). The improved conservation properties of this method may allow us to move away from the higher-order WENO discretizations presently used in the level set advancement and reinitialization equations. With lower-order methods, adaptation can be added in the region of the zero-level set, resulting in a further significant reduction in computational cost.

REFERENCES

Chandrasekhar, S. 1961 Hydrodynamic and Hydromagnetic Stability. *Oxford University Press.*

Chen, G., Kharif, C, Zaleski, S., & Li, J. 1999 Two-dimensional Navier-Stokes simulation of breaking waves. *Phys. Fluids* **11** no. 1, 121-133.

Enright, D., Fedkiw, R., Ferziger, J. & Mitchell, I. 2002 A hybrid particle level set method for improved interface capturing. *J. Comput. Phys.* **183**, 83-116.

Glimm, J., Grove, J. W., Li, X. L., Oh, W. & Sharp, D. H. 2001 A critical analysis of Rayleigh-Taylor growth rates. *J. Comput. Phys.* **169**, 652-677.

H. Haj-Hariri, Q. Shi, and A. Borhan 1997 Thermocapillary motion of deformable drops at finite reynolds and marangoni numbers. *Phys. Fluids* **9**, 845.

Ham, F. E., Lien, F. S. & Strong, A. B. 2002 A Cartesian grid method with transient anisotropic adaptation. *J. Comput. Phys.* **179**, 469-494.

Han, J. & Tryggvason, G. 1999a Secondary breakup of axisymmetric liquid drops. I. Acceleration by a constant body force. *Phys. Fluids* **11** no. 12, 3651-3667.

Han, J. & Tryggvason, G. 1999b Secondary breakup of axisymmetric liquid drops. II. Impulsive acceleration. *Phys. Fluids* **13** no. 6, 1554-1565.

Jiang, G-.S. & Peng, D. 2000 Weighted ENO schemes for Hamilton-Jacobi equations. *SIAM J. Sci. Comput.* **21** (6), 2126-2143.

Kim, D. & Choi, H. 2000 A Second-Order Time-Accurate Finite Volume Method for Unsteady Incompressible Flow on Hybrid Unstructured Grids. *J. Comput. Phys.* **162**, 411-428.

Lamb, H. 1932 Hydrodynamics. *Cambridge University Press.*

Osher, S. & Fedkiw, R. 2001 Level set methods: an overview and some recent results. *J. Comput. Phys.* **169**, 463.

Schneider, M. B., Dimonte, G. & Remington, B. 1998 Large and small structure in Rayleigh-Taylor mixing. *Phys. Rev. Lett.* **80**, 3507-3510.

Sethian, J. 2001 Evolution, implementation, and application of level set and fast marching methods for advancing fronts. *J. Comput. Phys.* **169**, 503.

Sussman, M., Smereka, P. & Osher, S. 1994 A level set approach for computing solutions to incompressible two-phase flow. *J. Comput. Phys.* **114**, 146-159.

Mark Sussman, Ann S. Almgren, John B. Bell, Phillip Colella, Louis H. Howell, and Michael L. Welcome 1999 An Adaptive Level Set Approach for Incompressible Two-Phase Flows *J. Comput. Phys.* **148**, 81-124.

Young, Y.-N., Tufo, H., Dubey, A. & Rosner, R. 2001 On the miscible Rayleigh-Taylor instability: two and three dimensions. *J. Fluid Mech.* **447**, 377-408.